Methylolation of Melamine with Incipient Condensation. II. Mathematical Modeling

V. V. Nicolau,[1,2,3] D. A. Estenoz,[1] G. R. Meira[1]

[1]*INTEC (CONICET and U.N.L.), Güemes 3450, Santa Fe 3000, Argentina*
[2]*Centro S.A., San Francisco 2400, Córdoba, Argentina*
[3]*Departamento Química Fac. Reg. San Fco., U.T.N., San Francisco 2400, Córdoba, Argentina*

Received 25 September 2008; accepted 21 November 2008
DOI 10.1002/app.29728
Published online 2 April 2009 in Wiley InterScience (www.interscience.wiley.com).

ABSTRACT: A novel mathematical model is presented for the reaction between melamine (M) and formaldehyde (F) at pH = 9.0 and at temperatures between 38 and 90°C. It is based on a kinetic scheme that includes reversible methylolations, irreversible formation of (unsubstituted) methylene bridges, reversible formation of (unsubstituted) ether bridges, instantaneous dissolution of M, and instantaneous equilibrium for the hydration/dehydration of F. The model predicts the distributions of molecular weights and functionalities of the evolving MF resin. Arrhenius expressions were adjusted for the seven kinetic constants on the basis of measurements reported in the first part of this series. Even though the final products contain thousands of different molecular species, 21 of them constitute more than 90% of the total weights. During the initial period with negligible condensation, the undissolved M distorts the distributions of molecular weights and functionalities; but the reversibility of methylolations corrects for such distortion prior to the effective start of condensation. © 2009 Wiley Periodicals, Inc. J Appl Polym Sci 113: 1017–1029, 2009

Key words: resins; modeling; simulations; molecular weight distribution

INTRODUCTION

In spite of the commercial importance of melamine-formaldehyde (MF) resins, their synthesis is not completely understood. The difficulties include the presence of impurities and side reactions, the generation of a large number of molecular structures, the large effect of pH, and the initial system heterogeneity caused by the low water solubility of melamine (M).

Table I presents a typical mechanism for the reaction between formaldehyde (F) and M at low initial *F* : *M* ratios. It includes the physical dissolution of M (that is loaded into the reactor as a solid powder)[1]; the hydration/dehydration of F[2]; two reversible methylolations[3]; an irreversible formation of unsubstituted methylene bridges[4–6]; and a reversible formation of unsubstituted ether bridges.[5,6] Not included in Table I are intramolecular reactions or the formation of (mono- or disubstituted) condensation bridges. Substituted (methylene or ether) bridges are not included because of the low initial F : M ratios together with the lower reactivity of monosubstituted amines.[7]

Condensation is negligible at temperatures below 60°C and pH between 9 and 10.[3,8] Gordon et al.[3] proposed a general reaction scheme for the methylolation/demethylolation without condensation that involves the generation of nine single-ringed methylolmelamines (Fig. 1). For such mechanism, Tomita[8] adjusted 14 (out of the 24) kinetic constants on the basis of dilute solution reactions carried out in at 48°C and pH = 9. Based on the same measurements[8] and reaction scheme,[3] all the 24 methylolation/demethylolation kinetic constants were recently adjusted in Nicolau et al.[9]

Okano and Ogata[4] investigated a series of methylolation/condensations of M and F at 35, 40, and 70°C; and pH in the range 3–10.6. Nastke et al.[5] presented a theoretical and experimental investigation on buffered methylolation/condensations. In the first part of this series,[10] five reactions between F and M were carried out, and the main results are presented further below. Gupta[11] employed 10 "chemical entities" for modeling a batch reaction between M and F. The models assume 12 irreversible methylolations, 13 irreversible methylene bridge formations, and only five kinetic constants. The model produces a gross estimate of the average number of rings per molecule.[11] Kumar and Chandra[12] extended the model by Gupta,[11] by assuming either irreversible

Correspondence to: G. R. Meira (gmeira@santafe-conicet.gov.ar).

Contract grant sponsors: Centro S.A, CONICET, U.N.L, SeCYT.

TABLE I
Global Kinetic Mechanism

Dissolution of M:

$$M_{Solid} \longrightarrow M_{Diss.} \quad (1)$$

Hydration/Dehydration of F:

$$CH_2O + H_2O \underset{kd}{\overset{k_h}{\rightleftarrows}} HOCH_2OH \quad (2)$$

Methylolations:

$$—NH_2 + CH_2O \underset{k'_{m_1}}{\overset{k_{m_1}}{\rightleftarrows}} — NHCH_2OH \quad (3)$$

$$—NHCH_2OH + CH_2O \underset{k'_{m_2}}{\overset{k_{m_2}}{\rightleftarrows}} — N(CH_2OH))_2 \quad (4)$$

Condensations:

$$—NH_2 + — NHCH_2OH \xrightarrow{k_{MB}} — NHCH_2NH — + H_2O \quad (5)$$

$$2\ —NHCH_2OH \underset{k'_{EB}}{\overset{k_{EB}}{\rightleftarrows}} — NHCH_2OCH_2NH — + H_2O \quad (6)$$

methylolations with reversible condensations or reversible methylolations with irreversible condensations; and adjusted the five associated kinetic constants on the basis of the mentioned measurements by Tomita.[8] Kumar and Katiyar[13] readjusted the models by Kumar and Chandra[12] on the basis of

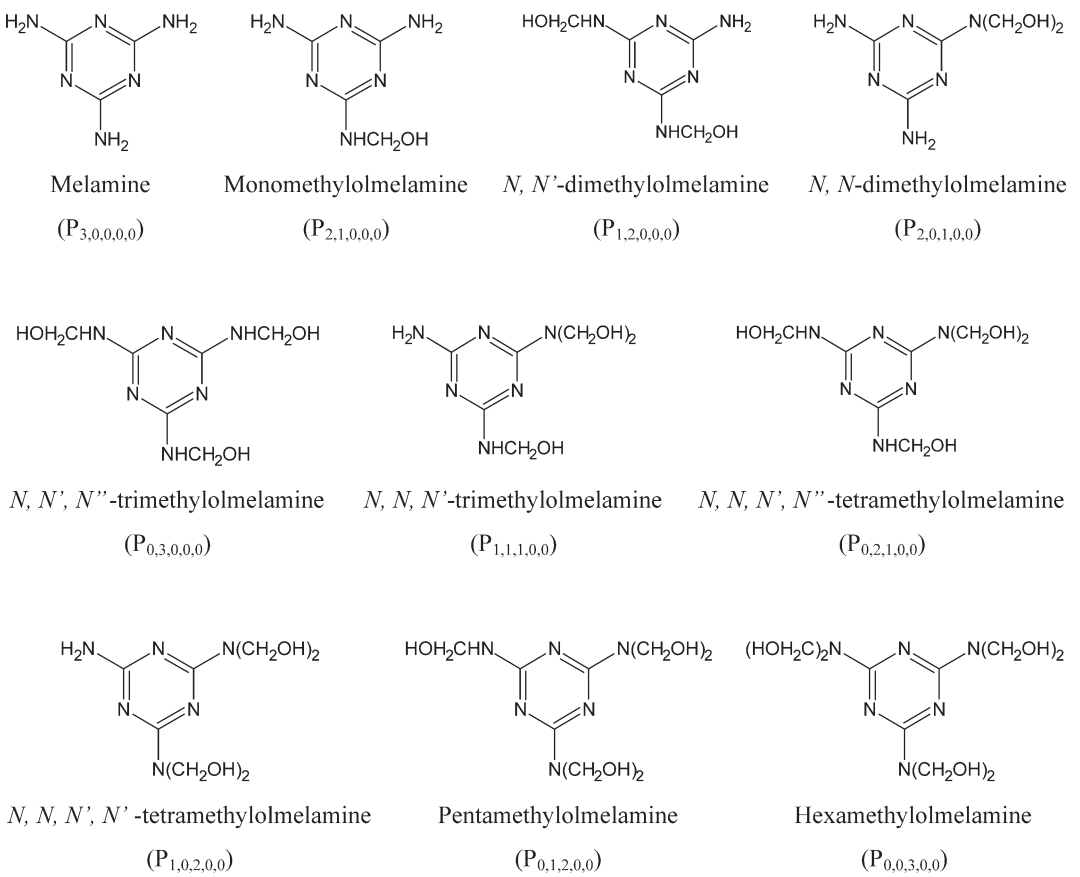

Figure 1 Melamine and its nine (single-ringed) methylolated species.[3] Between parentheses are the symbols of the adopted nomenclature.

TABLE II
Global Kinetic Constants for the Reaction between M and F at pH ≅ 9, Temperatures of 35, 48, 50, and 70°C, and with $[H_2O]$ = 47–55 mol/L

	T (°C)	$[F_T]^\circ/[M_T]^\circ$	k^*_m (L/mol s)	k_m (L/mol s)	k'_m (s^{-1})	k_{MB} (L/mol s)	k_{EB} (L/mol s)	k'_{EB} (s^{-1})
Methylolation only								
•Okano and Ogata[4]	35	2.0	1.89×10^{-4}	2.20[a]	–	–	–	–
•Gordon et al.[3]	35	3.0	1.08×10^{-4}[b]	2.51[a]	2.27×10^{-5}[c]	–	–	–
	48	3.0	5.14×10^{-4}[b]	8.52[a]	1.33×10^{-4}[c]	–	–	–
	50	3.0	6.46×10^{-4}[b]	10.20[a]	1.72×10^{-4}[c]	–	–	–
	70	3.0	5.51×10^{-3}[b]	54.61[a]	1.94×10^{-3}[c]	–	–	–
•Nicolau et al.[9]	48	1.0–30.0	–	7.12[a]	9.81×10^{-5}	–	–	–
Methylolation/condensation								
•Nastke et al.[5]	50	1.0	5.24×10^{-4}	7.05[d]	1.14×10^{-4}	2×10^{-6}	2.09×10^{-2}	3.63×10^{-4}
	50	3.0	1.82×10^{-3}	26.94[e]	3.69×10^{-4}	2×10^{-6}	5.37×10^{-3}	2.09×10^{-4}
	70	1.0	1.2×10^{-3}	10.14[d]	2.70×10^{-4}	4×10^{-6}	3.89×10^{-2}	6.96×10^{-4}
	70	3.0	5.01×10^{-3}	46.57[e]	9.48×10^{-4}	3.2×10^{-5}	8.91×10^{-3}	6.61×10^{-4}
•This work	35	2.0	–	2.88	1.64×10^{-5}	2.01×10^{-7}	5.49×10^{-8}	1.65×10^{-8}
	48	2.0	–	5.64	5.61×10^{-5}	5.13×10^{-7}	2.66×10^{-7}	4.87×10^{-8}
	50	2.0	–	6.22	6.73×10^{-5}	5.89×10^{-7}	3.35×10^{-7}	5.71×10^{-8}
	70	2.0	–	15.7	3.81×10^{-4}	2.13×10^{-6}	2.93×10^{-6}	2.51×10^{-7}

Previously-reported values[3–5,9] are compared with estimates obtained in this work.
[a] Estimate of eq. (8) with $[H_2O]$ = 55 mol/L.
[b] Calculated from k^*_m (L/mol s) = $6 \times 10^{12}\, e^{-11876/T}$ (298–328°K).
[c] Calculated from k'_m (s^{-1}) = $2 \times 10^{14}\, e^{-13436/T}$ (298–328°K).
[d] Estimate of eq. (8) with $[H_2O]$ = 47 mol/L.
[e] Estimate of eq. (8) with $[H_2O]$ = 52 mol/L.

new measurements from a single variable, the total formaldehyde concentration.

This work presents a novel mathematical model for the synthesis of MF resins. As far as the authors are aware, this is the first model that estimates the distributions of molecular weights and functionalities of the evolving oligomers mixture.

GENERAL CONSIDERATIONS

For reactions at pH = 9, temperatures of 35, 48, 50, and 70°C, and water concentrations between 47 and 55 mol/L, Table II reproduces some previous estimates of the main global kinetic constants.[3–5,9] Except for the last-cited article, Refs. 3–5 assumed a global methylolation:

$$—H + CH_2O \underset{k'_m}{\overset{k_m}{\rightleftarrows}} — CH_2OH \qquad (7)$$

Furthermore, the forward methylolation constants of Refs. 3–5 (reproduced in Table II under k_m*) were estimated from measurements of the total F concentration ($[F_T] = [CH_2O] + [HOCH_2OH]$), rather than of $[CH_2O]$. The kinetic constants reported by Nastke et al.[5] were assumed to depend on the initial F : M ratio. The values under k_m* were corrected to take into consideration that only COH_2 undergoes methylolation. The corrected constants (k_m in Table II) were obtained through[9]:

$$k_m = k^*_m(1 + K_{MG}[H_2O]), \quad \text{with} \quad K_{MG} = k_h/k_d = e^{-2.325+2579/T} \qquad (8)$$

where eq. (8) assumes an instantaneous equilibrium for eq. (2). In the case of k_m under Okano and Ogata,[4] a factor of 0.5 was also included in the right hand-side of eq. (8), to allow for the methylolation of all six reactive H's of M. Finally, the values of k_m and k'_m under Nicolau et al.[9] were obtained by averaging the (12 forward and 12 backward) reported constants.

Consider the five reactions between M and F described in the first part of this series.[10] All the reactions were at pH = 9.0, and with a common initial concentrations ratio $[F_T]^\circ/[M_T]^\circ$ of 2. In Exps 1–5, the reaction temperatures were 38, 48, 60, 70, and 90°C, respectively. Except for Exp. 5, all the other reactions were initially heterogeneous. The final results are in Figures 2 and 3, and in Table III. Figure 2(a–e) present the evolutions of $[F_T]$ and ($[F_T]$ + [—CH_2OH]), as determined by volumetric techniques. The rate of consumption of F_T increases with the temperature. In Exps 1 and 2, condensation was almost negligible, and $[F_T]$ and ($[F_T]$ + [—CH_2OH]) reach quasi-equilibrium values. In the final periods of Exps 3–5, the slow fall of $[F_T]$ + [$-CH_2OH$] is indicative of

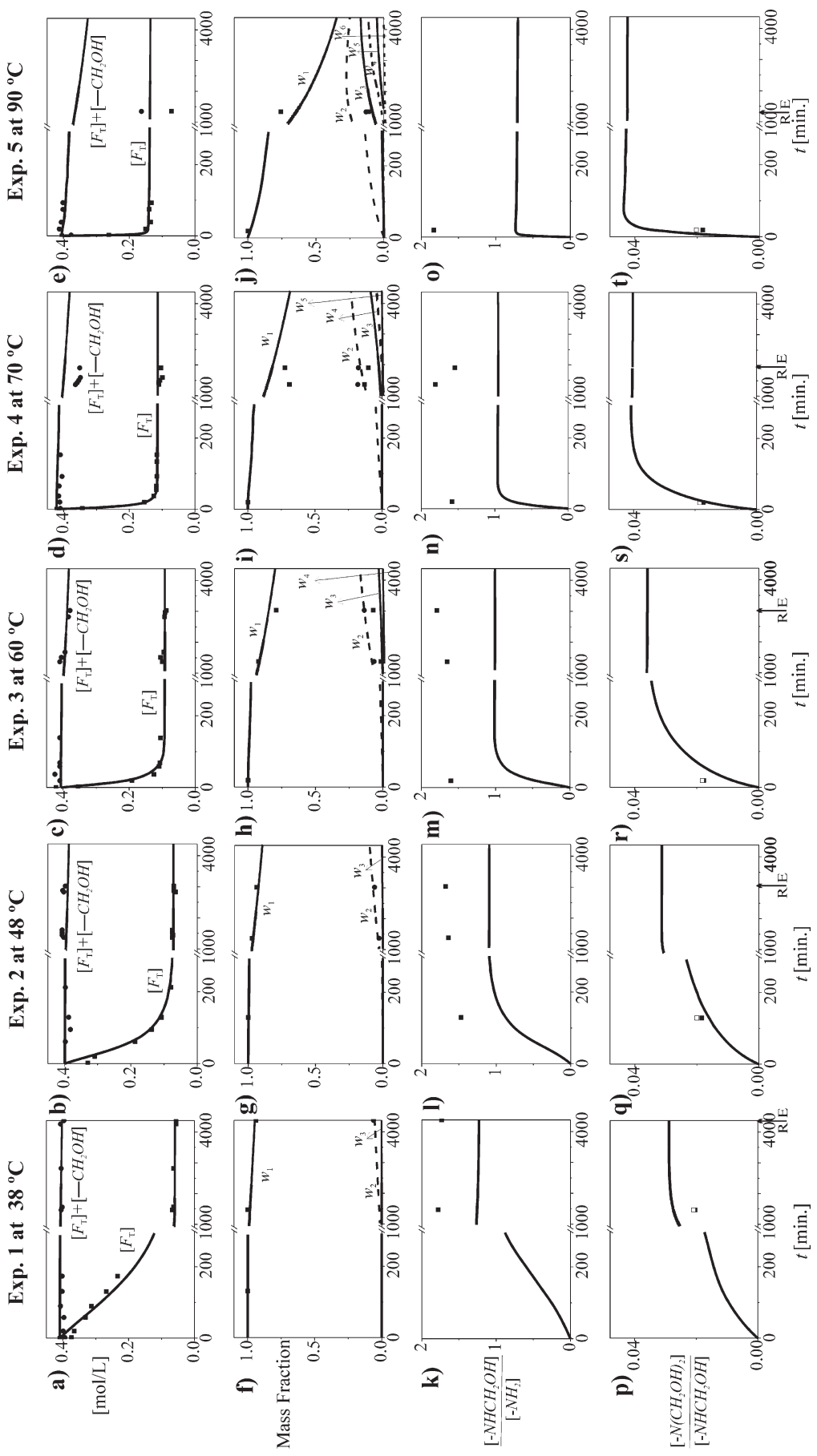

Figure 2 Direct measurements (in symbols) reproduced from Nicolau et al.[10] for reactions between M and F at pH = 9.0, $[F_T]^\circ/[M_T]^\circ = 2$, and temperatures of 38, 48, 60, 70, and 90°C. (a)–(e) Evolutions of $[F_T]$ and $[F_T]+[-CH_2OH]$). (f)–(j) Mass fractions of species with 1-, 2-, and 3-or-more azine rings per molecule w_i ($i = 1, 2, 3$). (k)–(o) Ratio of secondary to primary amines. (p)–(t) Ratio of tertiary to secondary amines, where the open and solid symbols correspond to ^{1}H-NMR measurements of $[-N(\boldsymbol{CH_2}OH)_2]$: $[-NH\boldsymbol{CH_2}OH]$ and $[-N(CH_2\boldsymbol{OH})_2]$: $[-NHCH_2\boldsymbol{OH}]$, respectively. RE, reaction end. Also shown, are the new model predictions (in continuous or dashed trace).

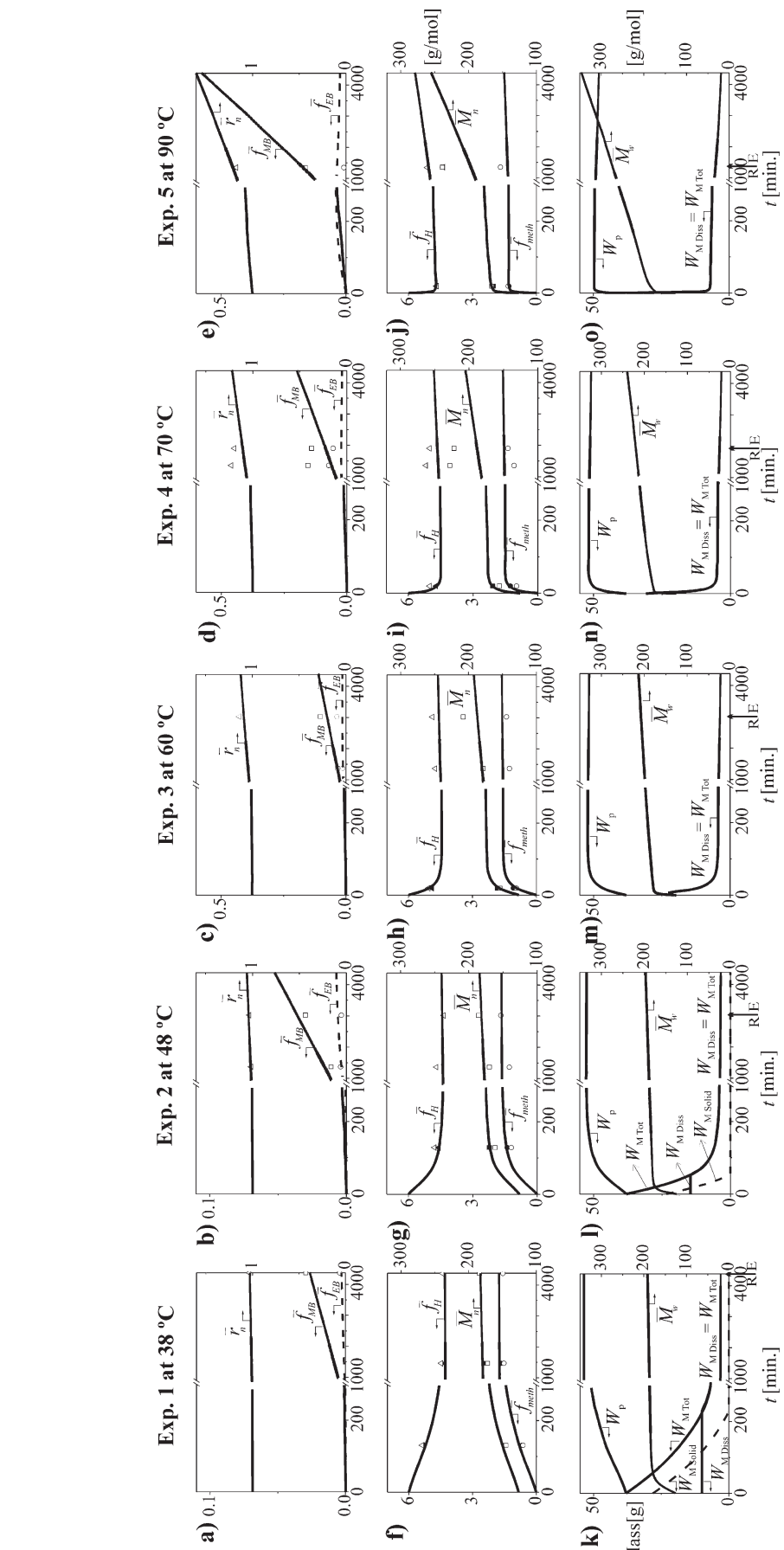

Figure 3 Indirect measurements (in symbols) reproduced from Nicolau et al.[10] for reactions between M and F at pH = 9.0, $[F_T]^\circ/[M_T]^\circ = 2$, and temperatures of 38, 48, 60, 70, and 90°C. (a)–(e) Average functionalities of methylene and ether bridges and number-average chain length. (f)–(j) Number-average molecular weights and average functionalities. Symbols: $\bar{f}_H$: △,▲; $\bar{f}_{meth}$: ○,●; $\bar{M}_n$: □,■ (the solid symbols indicate volumetric measurements, and the open symbols indicate combined SEC/volumetric measurements). (k)–(o) Masses of total ringed molecules (W_P), total M, dissolved M, undissolved M, and weight-average molecular weights. RE, reaction end. Also shown, are the new model predictions (in continuous or dashed trace).

TABLE III
Reactions Between M and F at pH = 9.0 and $[F_T]^\circ/[M_T]^\circ = 2$

Exp. no	T (°C)	Time (min)	$\bar{f}_H$	$\bar{f}_{meth}$	$\bar{f}_{MB} + \bar{f}_{EB}$	$\bar{M}_n$
1	38	4375	4.42 (4.37)	1.57 (1.71)	0.0337 (0.0360)	184 (182)
2	48	3025	4.36 (4.50)	1.69 (1.61)	0.0337 (0.0534)	186 (182)
3	60	3030	4.88 (4.66)	1.41 (1.57)	0.139 (0.115)	208 (189)
4	70	1905	5.01 (4.75)	1.39 (1.53)	0.196 (0.137)	222 (192)
5	90	1350	4.38 (5.21)	1.69 (1.34)	0.172 (0.271)	239 (205)

Measurements reproduced from Nicolau et al.,[10] and model predictions obtained in this work (in parentheses).

condensation. Figure 2(f–j) shows the weight fractions of species with 1-,2-, and 3-or-more azine rings per molecule, as determined by size exclusion chromatography (SEC). In Exps 1 and 2, the final products essentially consisted of single-ringed species (see columns 4–6 of Table III). In contrast, moderate amounts of 2- and 3-or-higher ringed species were produced in Exps 3–5. In all cases, the mass fraction of single-ringed species is larger than the added mass fractions of species with two or more rings. As determined by ^{1}H-NMR, Figure 2(k–o) and 2(p–t), respectively, present the ratios of secondary to primary amines ([—$N\boldsymbol{H}CH_2OH$] : [—$N\boldsymbol{H}_2$]), and of tertiary to secondary amines ([—$N(C\boldsymbol{H}_2OH)_2$] : [—$NHC\boldsymbol{H}_2OH$] and [—$N(CH_2O\boldsymbol{H})_2$] : [—$NHCH_2O\boldsymbol{H}$]). Obtained from SEC/titration measurements, Figure 3(a–j) shows (indirect and potentially erroneous) estimates of the following averages: number-average number of methylene and ether bridges per molecule ($\bar{f}_{MB}$ and $\bar{f}_{EB}$, respectively); number-average molecular weights ($\bar{M}_n$); average number of reactive H's and methylols per molecule ($\bar{f}_H$and$\bar{f}_{meth}$, respectively); and number-average number of rings per molecule (or number-average chain length ($\bar{r}_n$), obtained from: $\bar{f}_{MB} + \bar{f}_{EB} + 1$. For the samples with negligible condensation and on the basis on titration measurements, Figure 3(f–j) also present estimates of $\bar{M}_n$, $\bar{f}_H$, and $\bar{f}_{meth}$ (in solid symbols). In all the reactions, $\bar{f}_{MB}$ and $\bar{r}_n$ increase monotonically, and $\bar{f}_{MB} > \bar{f}_{EB}$. In Exps 1 and 2 with negligible condensation, the values of $\bar{r}_n$ remain close to unity, whereas $\overline{M}_n$ increases moderately because of methylolation, from 126 g/mol (the molar mass of M). In Exps 3–5, both $\bar{r}_n$ and $\bar{M}_n$ increase because of condensation. Table III presents the product characteristics at the final reaction times indicated by arrows in Figures 2 and 3. As a consequence of the negligible condensation and the common initial ratios $[F_T]^\circ : [M_T]^\circ = 2$, the final methylol functionalities of

TABLE IV
Detailed Kinetic Mechanism

Dissolution of M:

$$P_{3,0,0,0,0\text{Solid}} \longrightarrow P_{3,0,0,0,0\text{Diss.}} \tag{9}$$

Hydration/dehydration of F:

$$F + H_2O \underset{k_d}{\overset{k_h}{\rightleftarrows}} HOCH_2OH \tag{10}$$

Methylolations:

$$P_{A_0+1,A_1-1,A_2,M_0,E_0} + F \underset{k'_{m_1}}{\overset{k_{m_1}}{\rightleftarrows}} P_{A_0,A_1,A_2,M_0,E_0} \tag{11}$$

$$P_{A_0,A_1+1,A_2-1,M_0,E_0} + F \underset{k'_{m_2}}{\overset{k_{m_2}}{\rightleftarrows}} P_{A_0,A_1,A_2,M_0,E_0} \tag{12}$$

Condensations:

$$P_{A'_0,A'_1,A'_2,M'_0,E'_0} + P_{A_0-A'_0+1,A_1-A'_1+1,A_2-A'_2,M_0-M'_0-1,E_0-E'_0} \xrightarrow{k_{MB}} P_{A_0,A_1,A_2,M_0,E_0} + H_2O \tag{13}$$

$$P_{A'_0,A'_1,A'_2,M'_0,E'_0} + P_{A_0-A'_0,A_1-A'_1+2,A_2-A'_2,M_0-M'_0,E_0-E'_0-1} \underset{k'_{EB}}{\overset{K_{EB}}{\rightleftarrows}} P_{A_0,A_1,A_2,M_0,E_0} + H_2O \tag{14}$$

with (A_0, A_0', A_1, A_1', A_2, A_2', M_0, M_0', E_0, $E_0' = 0, 1, 2, \ldots$)

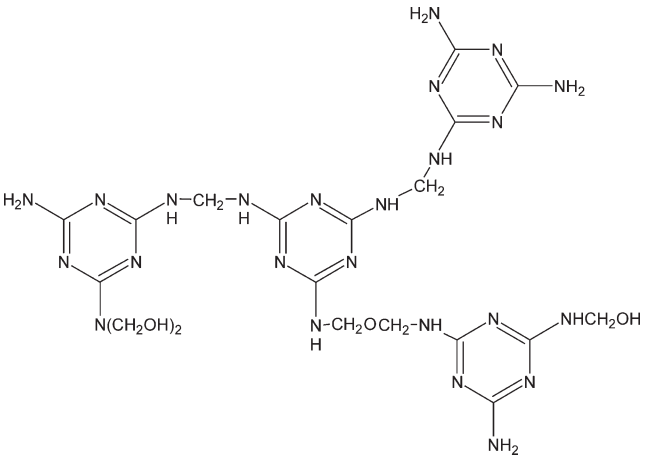

Figure 4 One possible configuration of species $P_{A_0,A_1,A_2,M_0,E_0} = P_{4,1,1,2,1}$, where $A_0 = 4$ is the number of $-NH_2$ groups; $A_1 = 1$ is the number of $-NHCH_2OH$ groups; $A_2 = 1$ is the number of $-NH(CH_2OH)_2$ groups; $M_0 = 2$ is the number of methylene bridges; and $E_0 = 1$ is the number of ether bridges.

Exps 1 and 2 resulted $\bar{f}_{meth} = 1.57$ and 1.69, respectively. In contrast, in Exps 3–5, somewhat increased final values of $\bar{f}_H$ and $\bar{f}_{meth}$ are observed (Fig. 3).

MATHEMATICAL MODEL

Consider the detailed kinetics of Table IV. Equations (9–14) are equivalent to eqs. (1–6), except for the fact that any M-based molecule is characterized by P_{A_0,A_1,A_2,M_0,E_0}; where A_0, A_1, and A_2 are the number of primary, secondary, and tertiary amines [$-NH_2$, $-NHCH_2OH$, and $-N(CH_2OH)_2$, respectively]; and M_0 and E_0 are the number of unsubstituted methylene and ether bridges ($-NHCH_2NH-$ and $-NHCH_2OCH_2NH-$, respectively). Figure 4 illustrates a hypothetical isomer of $P_{4,1,1,2,1}$. Figure 1 shows the nomenclature of the 10 possible single-ringed species according to Gordon et al.[3] Note that Melamine is included as a special case of P_{A_0,A_1,A_2,M_0,E_0}. Also note that the 10 possible single-ringed species only exhibit seven different molar masses. For topologies containing from 1 to 12 azine rings, Table V presents the total numbers of different P_{A_0,A_1,A_2,M_0,E_0} species and of different molar mass types. From a total of 5785 P_{A_0,A_1,A_2,M_0,E_0} species with up to 12 rings, only 282 of them exhibit different molar mass types (Table V).

The mathematical model is presented in the Appendix. The basic assumptions are: (a) constant reaction volume; (b) instantaneous equilibrium of eq. (10); and (c) instantaneous dissolution of M, with a concentration of dissolved M identical to the solubility of M in pure water.[14] Equations (A3)–(A6) represent the mass balances of F, methylene glycol, water, and all the possible P_{A_0,A_1,A_2,M_0,E_0} species (including M). The distributions of molecular weights and functionalities are calculated from the mass of all the different P_{A_0,A_1,A_2,M_0,E_0} species. The computer program was written in Fortran Power Station. The differential equations were integrated by means of a finite difference procedure that adopted a fixed time increment of 1 s. After a few seconds of simulation time,

TABLE V
Final Product Characteristics of Exps 1–5: Weight Percentages of Molecular Species with 1-, 2-,... 12-Rings Per Molecule, Weight-Average Molecular Weights, and Polydispersity Indexes

N° rings per molecule	N° of different P_{A_0,A_1,A_2,M_0,E_0} species[a]	N° of species with different values of M[b]	Exp. 1 (38°C). sample at 4375 min.	Exp. 2 (48°C). sample at 3025 min.	Exp. 3 (60°C) sample at 3030 min.	Exp. 4 (70°C). sample at 1905 min.	Exp. 5 (90°C). sample at 1350 min.
1	10	7	93.49	90.48	81.19	78.1	63.1
2	30	10	6.12	8.72	15.81	18.0	24.9
3	63	13	0.374	0.736	2.53	3.26	8.06
4	112	16	2.23×10^{-2}	5.94×10^{-2}	0.401	0.585	2.63
5	180	19	1.32×10^{-3}	4.80×10^{-3}	6.52×10^{-2}	0.108	0.875
6	270	22	–*	3.93×10^{-4}	1.09×10^{-2}	2.03×10^{-2}	0.298
7	385	25	–*	–*	1.88×10^{-3}	3.93×10^{-3}	0.103
8	528	28	–*	–*	3.53×10^{-4}	7.74×10^{-4}	3.63×10^{-2}
9	702	31	–*	–*	–*	1.55×10^{-4}	1.29×10^{-2}
10	910	34	–*	–*	–*	–*	4.68×10^{-3}
11	1155	37	–*	–*	–*	–*	1.78×10^{-3}
12	1440	40	–*	–*	–*	–*	8.72×10^{-4}
$\bar{M}_w$ (g/mol)			192	194	211	217	251
$\bar{M}_w/\bar{M}_n$			1.05	1.07	1.12	1.13	1.22

[a] Total No. of species: 5785.
[b] Total No. of species: 251.
* Value below 9×10^{-5}%.

TABLE VI
Model Parameters

	Exp. 1 at 38°C	Exp. 2 at 48°C	Exp. 3 at 60°C	Exp. 4 at 70°C	Exp. 5 at 90°C	Expressions T (°K)	References
K_{MG} (mol/L)	391	302	226	180	119	$e^{-2.325+2579/T}$	15
S^* (mol/L)	0.0526	0.0768	0.118	0.164	0.300	$0.0794\ (10^{-1642/T+5.101})$	14
k_{m_1} (L/mol s)	6.53	10.9	19.4	30.3	69.1	$9.22 \times 10^7\ e^{-5120/T}$; ($r^2 = 0.85$)	This work
	4.79	*10.2*	*36.6*	*32.0*	*50.5*		
k'_{m_1} (s^{-1})	1.83×10^{-5}	5.33×10^{-5}	1.77×10^{-4}	4.51×10^{-4}	2.51×10^{-3}	$1.51 \times 10^{10}\ e^{-10682/T}$; ($r^2 = 0.85$)	This work
	1.15×10^{-5}	*3.85×10^{-5}*	*7.02×10^{-4}*	*4.25×10^{-4}*	*1.48×10^{-3}*		
k_{m_2} (L/mol s)	0.225	0.370	0.645	0.996	2.21	$1.91 \times 10^6\ e^{-4962/T}$; ($r^2 = 0.51$)	This work
	0.0895	*0.485*	*1.47*	*2.09*	*0.875*		
k'_{m_2} (s^{-1})	2.56×10^{-5}	5.89×10^{-5}	1.50×10^{-4}	3.11×10^{-4}	1.18×10^{-3}	$1.06 \times 10^7\ e^{-8319/T}$; ($r^2 = 0.56$)	This work
	7.40×10^{-6}	*8.19×10^{-5}*	*3.42×10^{-4}*	*1.46×10^{-3}*	*2.75×10^{-4}*		
k_{MB} (L/mol s)	2.52×10^{-7}	5.13×10^{-7}	1.14×10^{-6}	2.13×10^{-6}	6.67×10^{-6}	$2.19 \times 10^3\ e^{-7118/T}$; ($r^2 = 0.93$)	This work
	2.69×10^{-7}	*3.58×10^{-7}*	*1.20×10^{-6}*	*3.61×10^{-6}*	*4.99×10^{-6}*		
k_{EB} (L/mol s)	7.99×10^{-8}	2.66×10^{-7}	1.02×10^{-6}	2.93×10^{-6}	2.01×10^{-5}	$4.60 \times 10^9\ e^{-12002/T}$; ($r^2 = 0.67$)	This work
	3.59×10^{-8}	*1.26×10^{-6}*	*4.55×10^{-7}*	*3.09×10^{-6}*	*1.37×10^{-10}*[a]		
k'_{EB} (s^{-1})	2.14×10^{-8}	4.87×10^{-8}	1.22×10^{-7}	2.51×10^{-7}	9.39×10^{-7}	$6.22 \times 10^3\ e^{-8209/T}$; ($r^2 = 0.17$)	This work
	2.60×10^{-9}	*1.15×10^{-6}*	–[b]	*8.73×10^{-8}*	–[b]		
min E_1 eq. (15a)	*0.0121*	*0.0241*	*0.0423*	*0.0279*	*0.0454*		
min E_2 eq. (16a)	*0.0507*	*0.0640*	*0.626*	*0.430*	*2.194*		
$K_{m_1} = k_{m_1}/k'_{m_1}$	3.57×10^5	2.05×10^5					This work
$K_{m_2} = k_{m_2}/k'_{m_2}$	8.78×10^3	6.27×10^3					This work

The final kinetic constants (in normal font) were calculated from the Arrhenius expressions. The kinetic constants in italics were adjusted with an optimization procedure for each of the Exps 1–5.
[a] Value discarded for the Arrhenius estimations.
[b] Discarded low negative value.

the program automatically generated all the possible P_{A_0,A_1,A_2,M_0,E_0} species with up to 12 rings per molecule.

Model parameters

The model parameters are presented in Table VI. The expressions for the equilibrium constant of F hydration/dehydration (K_{MG}) and for the water solubility of M (S^*) were directly taken from the literature.[14,15] The kinetic constants were all adjusted in this work, to fit the measurements of Figures 2 and 3(a–e).[10]

Detectable condensation starts well after reversible methylolations have reached equilibrium. This enabled a sequential adjustment of the model parameters. In the first step, Arrhenius expressions were adjusted for k_{m_1}, k_{m_2}, k'_{m_1}, and k'_{m_2}; taking into consideration only the initial periods with negligible condensation. In the second step, Arrhenius expressions were adjusted for k_{MB}, k_{EB}, and k'_{EB}; considering only the final periods with negligible methylolation. In Exps 1–5, the times for the ends of methylolation (or starts of condensation) were selected at 1470, 129, 19, 20, and 19 min, respectively.

In the first adjustment step, the measured variables were: $j_1 = [-N(C\boldsymbol{H}_2OH)_2] : [-NHC\boldsymbol{H}_2OH]$; $j_2 = [-N(CH_2O\boldsymbol{H})_2] : [-NHCH_2O\boldsymbol{H}]$; $j_3 = [-N\boldsymbol{H}CH_2OH] : [-N\boldsymbol{H}_2]$; $j_4 = [F_T]$; and $j_5 = [F_T]+[-CH_2OH]$. For each experiment, k_{m_1}, k_{m_2}, k'_{m_1}, and k'_{m_2} were adjusted by application of the following minimization algorithm:

$$\min_{(k_{m_1},k_{m_2},k'_{m_1},k'_{m_2})} E_1 = \sum_{m=1}^{5} f_m E_{m_i} \tag{15a}$$

$$E_{m_i} = \frac{1}{n_{m_i}} \sum_{\forall t_i} \left(\frac{j_m(t_i)_{\text{exp}} - j_m(t_i)_{\text{theor}}}{j_m(t_i)_{\text{exp}}} \right)^2; \quad (m = 1, \ldots, 5);\ (i = 1, \ldots n_m) \tag{15b}$$

where E_1 is a scalar error; f_m ($m = 1,\ldots, 5$) are weighting factors that consider the accuracy of the corresponding measurements; E_{m_i} ($m = 1,\ldots, 5$) are the average relative errors of each of the j_m variables; $j_m(t_i)_{\text{exp}}$ and $j_k(t_i)_{\text{theor}}$ are the measurements and model predictions, respectively; and n_m is the total number of discrete measurements of j_m. The following weighting factors were adopted: $f_1 = f_2 = f_4 = f_5 = 1$, and $f_3 = 0.1$. The lower value of f_3 was caused by the relatively larger errors expected in the measurements of $[-N\boldsymbol{H}CH_2OH] : [-N\boldsymbol{H}_2]$.[10] The results for k_{m_1}, k_{m_2}, k'_{m_1}, and k'_{m_2}, and E_1 obtained by application of eqs. (15) are in italics in Table VI. From such set of values, Arrhenius expressions were adjusted (Table VI), and their corresponding (interpolated) estimates are presented in normal type (Table VI).

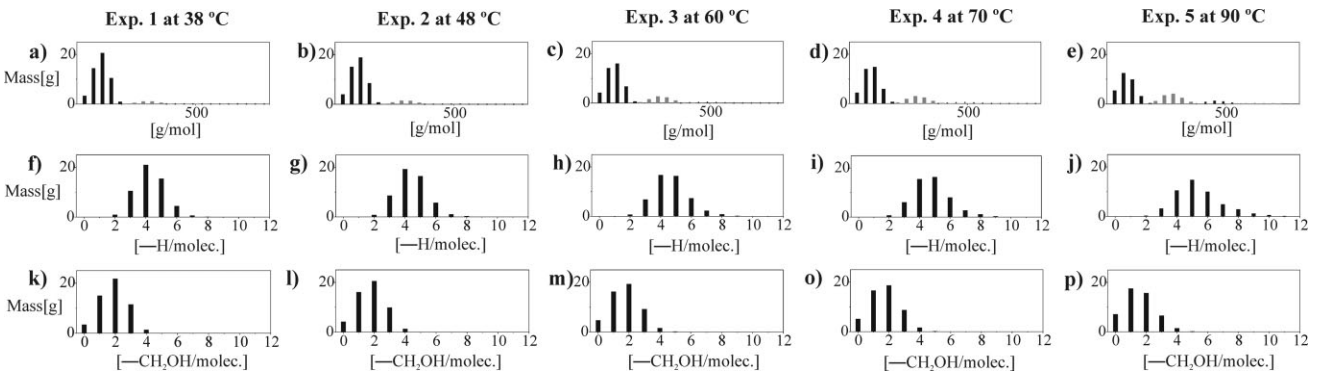

Figure 5 Model predictions for the final samples of Exps 1–5, taken at 4375, 3025, 3030, 1905, and 1350 min, respectively. (a)–(e) Distribution of molecular weights. (f)–(j) Distribution of reactive Hs/molecule (k)–(p) Distribution of methylols/molecule.

In the second adjustment step, the selected measurements were: j_3 = [—$N\boldsymbol{H}$CH$_2$OH] : [—$N\boldsymbol{H}_2$]; j_4 = [F_T]; j_5 = [F_T] + [—CH_2OH]; $j_6 = w_1$; $j_7 = w_2$; $j_8 = w_3$; j_9 = [—$HNCH_2NH$—]; and j_{10} = [—$HNCH_2OCH_2NH$—]; and the following algorithm was applied onto each of the five experiments:

$$\min_{(k_{MB}\ k_{EB}\ k'_{EB})} E_2 = \sum_{m=3}^{10} f_m E_{m_i} \tag{16a}$$

$$\text{with } E_{m_i} = \frac{1}{n_{m_i}} \sum_{\forall t_i} \left(\frac{j_m(t_i)_{exp} - j_m(t_i)_{theor}}{j_m(t_i)_{exp}} \right)^2; \quad (m = 3, \ldots, 10);\ (i = 1, \ldots n_m) \tag{16b}$$

The weighting factors were in this case: $f_4 = f_5 = f_6 = f_7 = f_8 = 1$, and $f_3 = f_9 = f_{10} = 0.1$. The lower values of f_9 and f_{10} are because of the large errors expected in the indirect estimations of the bridge concentrations. Table VI presents the final results for k_{MB}, k_{EB}, and k'_{EB}, and E_2 (in Italics), together with the derived Arrhenius expressions and corresponding interpolated values (in normal type). Note the relatively large value of E_2 for Exp. 5; possibly caused by the precipitate observed at the end of that reaction. Also, note the poor linear correlation for the Arrhenius of k'_{EB} ($r^2 = 0.17$). Possible reasons are errors in the bridge concentrations combined with numerical correlation between the adjusted constants (in particular, between the two forward condensation reactions, and between the forward and backward ether bridge formation constants).

For Exps 1 and 2 without condensation, the last two rows of Table VI show the methylolation/demethylolation equilibrium constants ($K_{m_1} = k_{m_1}/k'_{m_1}$ and $K_{m_2} = k_{m_2}/k'_{m_2}$); as calculated from the final interpolated values of K_{m_1}, k_{m_2}, k'_{m_1}, and K'_{m_2}. When the reaction temperature is increased from 38 to 48°C, the values of K_{m_1} and K_{m_2} decrease. This explains the higher final value of [F_T] in Exp. 2 with respect to Exp. 1 [Fig. 2(a,b)].

Crude estimates of the global methylolation/demethylolation constants k_m and k'_m were obtained by averaging the values of (k_{m_1}, k_{m_2}) and (k'_{m_1}, k'_{m_2}) presented in Table VI. Such averages are shown in Table II, together with the adjusted values of k_{MB}, k_{EB}, and k'_{EB}. Although the new estimate of k_m at 35°C is close to previous values,[3,4] larger differences are observed at 48, 50, and 70°C with respect to the values by Gordon et al.[3] The condensation constants adjusted in this work are lower than the values by Natske et al.[5] Possible reasons for this are: (a) the buffer solutions employed in Nastke et al.[5] and (b) the large experimental errors in the concentration of (methylene and ether) bridges.[10]

SIMULATION RESULTS

Figures 2 and 3(a–j), and Table III present the model predictions with experimental verification. In general, the simulation results are in reasonable agreement with the measurements. The larger differences are observed in the ratio of secondary to primary amines [Fig. 2(k–o)], and in the final product characteristics of Exp. 5. Simulation results suggest that molecules with up to seven or eight rings per molecule are present in potentially detectable amounts. In Exps 4 and 5, the average number of ether bridges per molecule ($\bar{f}_{EB}$) first increase, reach a maximum, and finally decrease. This final decrease is caused by a fall in the concentration of tertiary amines due to reversible methylolation [Fig. 3(d–e)].

Figure 3(k–o), Figure 5, and Tables V and VII present additional simulation results without experimental validation. Figure 3(k–o) show the predicted evolutions of: (a) the total mass (W_P); (b) the masses of total, dissolved, and undissolved M ($W_{M,Tot}$, $W_{M,Diss}$, and $W_{M,Solid}$, respectively), and (c) the weight-average molecular weight $\overline{M}_n$. The initial mass coincides with the total initial M mass. The total mass first rapidly increases due to methylolation, but then slowly decreases due to bridge

TABLE VII
Model Predictions for the Final Product of Exp. 5: Weight Percentage of the Most Abundant P_{A_0,A_1,A_2,M_0,E_0} Species

Rings/ molecule	P_{A_0,A_1,A_2,M_0,E_0}	Molar mass (g/mol)	Weight %
1	$P_{3,0,0,0,0}$ ($\equiv M$)	126	10.9
	$P_{2,1,0,0,0}$	156	25.2
	$P_{1,2,0,0,0}$	186	18.7
	$P_{2,0,1,0,0}$	186	1.27
	$P_{0,3,0,0,0}$	216	4.51
	$P_{1,1,1,0,0}$	216	1.84
	$P_{0,2,1,0,0}$	246	0.65
	Other	[246–306]	0.0762
2	$P_{4,0,0,1,0}$	264	2.39
	$P_{3,1,0,1,0}$	294	6.62
	$P_{2,2,0,1,0}$	324	6.82
	$P_{3,1,0,0,1}$	324	1.26
	$P_{1,3,0,1,0}$	354	3.09
	$P_{2,2,0,0,1}$	354	1.28
	$P_{2,1,1,1,0}$	354	0.63
	$P_{0,4,0,1,0}$	384	0.52
	$P_{1,3,0,0,1}$	384	0.58
	Other	[294–534]	1.70
3	$P_{4,1,0,2,0}$	432	1.62
	$P_{3,2,0,2,0}$	462	2.15
	$P_{2,3,0,2,0}$	492	1.43
	Other	[432–762]	2.88
4	$P_{4,2,0,3,0}$	600	0.63
	$P_{3,3,0,3,0}$	630	0.55
	Other	[540–990]	1.44
5–12		[708–2814]	1.30

formation. According to the model, Exps 1–4 exhibit initial heterogeneous periods, while Exp. 5 is homogeneous throughout. Heterogeneous periods are short in Exps 3 and 4, and cannot be visualized in Figure 3(m–n). In the heterogeneous periods of Exps 1 and 2, $W_{M,Solid} > 0$; whereas $W_{M,Diss}$ remains fixed at the water solubility of M [eq. (A2)]. After the heterogeneous periods, it remains: $W_{M,Diss} = W_{M,Tot}$. The model neglects the effects on the solubility of M of the other components (F, methylene glycol, and methylolated species). For this reason, errors are expected in $W_{M,Diss}$ and $W_{M,Solid}$.

The final product characteristics are in Figure 5 and in Tables III, V, and VII. Figure 5 show the weight-based distributions of: (i) molecular weights (a–e); (ii) H functionalities (f–j); and (iii) methylol functionalities (k–p); while their corresponding averages are given in Table III. In the MWDs of Figure 5(a–e), the contribution of single-ringed molecules is in black, of double-ringed molecules in gray, etc. Consider the results of Table V. In Exp. 5, the weight fraction of resin with six or more rings per molecule is below 1%. As expected, the final polydispersities $\bar{M}_w/\bar{M}_n$ increase with the molar mass and the reaction temperatures. Because of the relatively low initial F : M ratios, negligible amounts of highly methylolated single-ringed molecules are observed (Fig. 5). Table VII presents the detailed characteristics of the final product of Exp. 5. Even though the computer program calculated the amounts of all the possible P_{A_0,A_1,A_2,M_0,E_0} species with up to 12 rings per molecule, 21 of them account for more than 92% of the total weight (Table VII).

To investigate the effect of the initial heterogeneous periods on the final products of Exps 1 and 2, Table VIII compares the model predictions (after 5 min of reaction time and at the reaction ends), under two situations: (a) when admitting the heterogeneous periods; and (b) when assuming total dissolution of M from the beginning of the reactions. After 5 min of reaction time, large differences are observed in the model predictions according to whether or not M is assumed totally dissolved. However, such differences are negligible in the final product. This is because the heterogeneous periods are short with respect to the stage of methylolation/demethylolation without condensation; and during this stage the reversible methylolations conveniently redistribute the methylol substituents among the totally-dissolved single-ringed molecules.

CONCLUSIONS

For reactions between F and M carried out at pH = 9.0 and at temperatures between 38 and 90°C, a new mathematical model was developed that predicts the distributions of molecular weights and functionalities of the evolving reaction mixture. The kinetic

TABLE VIII
Exps 1 and 2: Model Predictions for the Product Characteristics after 5 min of Reaction Time and at the Reaction Ends Assuming an Initial Heterogeneous Period (First Result) and Model Predictions Assuming Total Dissolution of M from the Beginning of the Reaction (Second Results in Parenthesis)

Exp. No	Time (min.)	$\bar{M}_n$ (g/mol)	$\bar{f}_H$ (#/molecule)	$\bar{f}_{meth}$ (#/molecule)	$\bar{f}_{MB} + \bar{f}_{EB}$ (#/molecule)
1	5	127 (129)	5.97 (5.89)	0.0312 (0.111)	0.0000 (0.0000)
	4375	182 (183)	4.37 (4.37)	1.71 (1.71)	0.0360 (0.0360)
2	5	129 (133)	5.90 (5.78)	0.0983 (0.221)	0.0000 (0.0000)
	3025	182 (182)	4.50 (4.50)	1.61 (1.61)	0.0534 (0.0534)

constants of methylolation/demethylolation were adjusted to measurements along the initial stages of negligible condensation. The kinetic constants of bridge formation were adjusted to measurements along the final stages of effective condensation. Biases were expected in the adjusted parameters, due to measurement errors and to numerical correlation between the adjusted constants. In particular, improved measurements of bridge concentration would be required for more accurate estimates of the condensation constants.

In the initial heterogeneous periods, H and methylol groups become unevenly-distributed among the M molecules. However, such periods are short with respect to the reversible methylolations stage, thus enabling a convenient redistribution of the methylol substituents prior to the effective start of condensation. This self-correction mechanism is rather fortunate as it reduces the heterogeneity of the final distributions of molecular weights and functionalities.

In the third part of this series, the model is extended to simulate an industrial nonisothermal process in the presence of methanol. With minor changes, this model is extendable to the synthesis of other prepolymers such as urea-formaldehyde, phenol-formaldehyde, and polyurethanes.

NOMENCLATURE

F	CH_2O
F_T	Total formaldehyde [see eq. (A7)]
$\bar{f}_H$, $\bar{f}_{meth}$, $\bar{f}_{MB}$, $\bar{f}_{EB}$	Number-average functionalities of reactive H's, methylols, methylene bridges, and ether bridges
k_d	Rate constant of methylene glycol dehydration, s^{-1}
k_h	Rate constant of F hydration, L mol^{-1} s^{-1}
k_m	Global rate constant of methylolation, L mol^{-1} s^{-1}
k'_m	Global rate constant of demethylolation, s^{-1}
k_{m_1}, k_{m_2}	Primary and secondary rate constants of methylolation, L mol^{-1} s^{-1}
k'_{m_1}, k'_{m_2}	Primary and secondary rate constants of demethylolation, s^{-1}
k_{MB}, k_{EB}	Rate constants of methylene and ether bridge formation, $Lmol^{-1}$ s^{-1}
k'_{EB}	Backward rate constant of ether bridge formation, s^{-1}
K_{m_1}, K_{m_2}	Equilibrium constants of primary and secondary methylolation/demethylolation, L/mol
K_{MG}	Equilibrium constant for the hydration/dehydration of F, L/mol
M	Melamine
$M_{Diss.}$	Dissolved M
M_{Tot}	Total melamine [see eq. (A1)]
M_{Solid}	Undissolved M
$\overline{M}_n$, $\overline{M}_w$	Number- and weight-average molecular weights, g/mol
P_{A_0,A_1,A_2,M_0,E_0}	Ringed molecule containing A_0 unreacted amino groups, A_1 monohydroxymethylamino groups, A_2 dihydroxymethylamino groups, M_0 methylene bridges, and E_0 ether bridges
S^*	Solubility of M in pure water, mol/L
T	Time, s
T	Temperature, °C
[]	Molar concentration, mol/L

Superscripts

0	Initial condition

APPENDIX: MATHEMATHICAL MODEL

The total initial M is either dissolved (M_{Diss}) or as an undissolved solid powder (M_{Solid}), that is:

$$[M_{Tot}]^o = [M_{Diss.}]^o + [M_{Solid}]^o \quad \text{(A1)}$$

During the initial heterogeneous period, the concentration of dissolved M only depends on the temperature, and it coincides with the water solubility of M (in mol/L)[14]:

$$[M_{Diss.}] = S^* = 0.0794(10^{-1642/T+5.101}); \ ([M_{Solid}] > 0) \quad \text{(A2)}$$

From the detailed kinetic mechanism of Table IV, the following mass balances can be written for reagents and products:

$$\begin{aligned}\frac{d[F]}{dt} &= k_d[HOCH_2OH] \\ &+ k'_{m_1}\sum_{E_0=0}^{\infty}\sum_{M_0=0}^{\infty}\sum_{A_2=0}^{\infty}\sum_{A_1=0}^{\infty}\sum_{A_0=0}^{\infty}A_1\left[P_{A_0,A_1,A_2,M_0,E_0}\right] \\ &+ k'_{m_2}\sum_{E_0=0}^{\infty}\sum_{M_0=0}^{\infty}\sum_{A_2=0}^{\infty}\sum_{A_1=0}^{\infty}\sum_{A_0=0}^{\infty}A_2\left[P_{A_0,A_1,A_2,M_0,E_0}\right] \\ &- \Bigg\{k_h[H_2O] + .k_{m_1}\sum_{E_0=0}^{\infty}\sum_{M_0=0}^{\infty}\sum_{A_2=0}^{\infty}\sum_{A_1=1}^{\infty}\sum_{A_0=0}^{\infty}(A_0+1)\left[P_{A_0+1,A_1-1,A_2,M_0,E_0}\right] \\ &+ k_{m_2}\sum_{E_0=0}^{\infty}\sum_{M_0=0}^{\infty}\sum_{A_2=1}^{\infty}\sum_{A_1=0}^{\infty}\sum_{A_0=0}^{\infty}(A_1+1)[P_{A_0,A_1+1,A_2-1,M_0,E_0}]\Bigg\}[F]\end{aligned} \quad \text{(A3)}$$

$$\frac{d[HOCH_2OH]}{dt} = k_h[H_2O][F] - k_d[HOCH_2OH] \quad \text{(A4)}$$

$$\frac{d[H_2O]}{dt} = k_d[HOCH_2OH] + k_{MB}\sum_{E_0=0}^{\infty}\sum_{M_0=0}^{\infty}\sum_{A_2=0}^{\infty}\sum_{A_1=0}^{\infty}\sum_{A_0}^{\infty}\sum_{A_0'=0}^{A_0}\sum_{A_1'=1}^{A_1+1}\sum_{A_2'=0}^{A_2}\sum_{M_0'=0}^{M_0}\sum_{E_0'=0}^{E_0} A_1'\left[P_{A_0',A_1',A_2',M_0',E_0'}\right]$$
$$\times (A_0 - A_0' + 1)\left[P_{A_0-A_0'+1,A_1-A_1'+1,A_2-A_2',M_0-M_0'-1,E_0-E_0'}\right]$$
$$+ k_{EB}\sum_{E_0=0}^{\infty}\sum_{M_0=0}^{\infty}\sum_{A_2=0}^{\infty}\sum_{A_1=1}^{\infty}\sum_{A_0=0}^{\infty}\sum_{A_0'=0}^{A_0}\sum_{A_1'=1}^{A_1+1}\sum_{A_2'=0}^{A_2}\sum_{M_0'=0}^{M_0}\sum_{E_0'=0}^{E_0} A_1'\left[P_{A_0',A_1',A_2',M_0',E_0'}\right] \quad \text{(A5)}$$
$$\times (A_1 - A_1' + 2)\left[P_{A_0-A_0',A_1-A_1'+2,A_2-A_2',M_0-M_0',E_0-E_0'-]}\right]$$
$$-\left\{k_h[F] + k'_{EB}\sum_{E_0=0}^{\infty}\sum_{M_0=0}^{\infty}\sum_{A_2=0}^{\infty}\sum_{A_1=0}^{\infty}\sum_{A_0=0}^{\infty} E_0\left[P_{A_0,A_1,A_2,M_0,E_0}\right]\right\}[H_2O]$$

$$\frac{d[P_{A_0,A_1,A_2,M_0,E_0}]}{dt} = \{k_{m_1}(A_0+1)[P_{A_0+1,A_1-1,A_2,m_0,E_0}]$$
$$+ k_{m_2}(A_1+1)[P_{A_0,A_1+1,A_2-1,M_0,E_0}]\}[F]$$
$$+ k_{MB}\sum_{A_0'=0}^{A_0}\sum_{A_1'=1}^{A_1+1}\sum_{A_2'=0}^{A_2}\sum_{M_0'=0}^{M_0}\sum_{E_0'=0}^{E_0} A_1'[P_{A_0',A_1',A_2',M_0',E_0'}](A_0 - A_0' + 1)$$
$$\times [P_{A_0-A_0'+1,A_1-A_1'+1,A_2-A_2',M_0-M_0'-1,E_0-E_0'}]$$
$$+ k_{EB}\sum_{A_0'=0}^{A_0}\sum_{A_1'=1}^{A_1+1}\sum_{A_2'=0}^{A_2}\sum_{M_0'=0}^{M_0}\sum_{E_0'=0}^{E_0} A_1'[P_{A_0',A_1',A_2',M_0',E_0'}](A_1 - A_1' + 2)$$
$$\times [P_{A_0-A_0'+1,A_1-A_1'+2,A_2-A_2',M_0-M_0'-1,E_0-E_0'-1}]$$
$$-\left\{k'_{m_1}A_1 + k'_{m_2}A_2 + k'_{EB}[H_2O]E_0\right\}[P_{A_0,A_1,A_2,M_0,E_0}]$$
$$\text{(with) } A_0, A_0', A_1, A_1', A_2, A_2', M_0, M_0', E_0, E_0' = 1, 1, 2, \ldots) \quad \text{(A6)}$$

Assuming an instantaneous equilibrium for eq. (10), the total formaldehyde is:

$$[F_T] = [F] + [HOCH_2OH] \quad \text{(A7)}$$

and therefore[9]:

$$[F_T] = [F](1 + K_{MG}[H_2O]); \quad \text{with } K_{MG} = k_h/k_d \quad \text{(A8)}$$

where K_{MG} is the equilibrium constant of hydration/dehydration of F.[15] Taking the derivative of eqs. (A3) with respect to time, and replacing eq. (A7), it yields:

$$\frac{d[F_T]}{dt} = k'_{m_1}\sum_{E_0=0}^{\infty}\sum_{M_0=0}^{\infty}\sum_{A_2=0}^{\infty}\sum_{A_1=0}^{\infty}\sum_{A_0=0}^{\infty} A_1[P_{A_0,A_1,A_2,M_0,E_0}]$$
$$+ k'_{m_2}\sum_{E_0=0}^{\infty}\sum_{M_0=0}^{\infty}\sum_{A_2=0}^{\infty}\sum_{A_1=0}^{\infty}\sum_{A_0=0}^{\infty} A_2[P_{A_0,A_1,A_2,M_0,E_0}]$$
$$-\left\{k_{m_1}\sum_{E_0=0}^{\infty}\sum_{M_0=0}^{\infty}\sum_{A_2=0}^{\infty}\sum_{A_1=0}^{\infty}\sum_{A_0=0}^{\infty}(A_0+1)[P_{A_0+1,A1-1,A_2,M_0,E_0}]\right.$$
$$\left.+ k_{m_2}\sum_{E_0=0}^{\infty}\sum_{M_0=0}^{\infty}\sum_{A_2=0}^{\infty}\sum_{A_1=0}^{\infty}\sum_{A_0=0}^{\infty}(A_1+1)[P_{A_0,A_1+1,A_2-1,M_0,E_0}]\right\}[F] \quad \text{(A9)}$$

The average molecular weights of the evolving MF resin (that includes M as a special case) are:

$$\bar{M}_n = \frac{\sum_{E_0=0}^{\infty}\sum_{M_0=0}^{\infty}\sum_{A_2=0}^{\infty}\sum_{A_1=0}^{\infty}\sum_{A_0=0}^{\infty}[P_{A_0,A_1,A_2,M_0,E_0}]M_{P_{A_0,A_1,A_2,M_0,E_0}}}{\sum_{E_0=0}^{\infty}\sum_{M_0=0}^{\infty}\sum_{A_2=0}^{\infty}\sum_{A_1=0}^{\infty}\sum_{A_0=0}^{\infty}[P_{A_0,A_1,A_2,M_0,E_0}]} \quad \text{(A10)}$$

$$\bar{M}_w = \frac{\sum_{E_0=0}^{\infty}\sum_{M_0=0}^{\infty}\sum_{A_2=0}^{\infty}\sum_{A_1=0}^{\infty}\sum_{A_0=0}^{\infty}[P_{A_0,A_1,A_2,M_0,E_0}]M^2_{P_{A_0,A_1,A_2,M_0,E_0}}}{\sum_{E_0=0}^{\infty}\sum_{M_0=0}^{\infty}\sum_{A_2=0}^{\infty}\sum_{A_1=0}^{\infty}\sum_{A_0=0}^{\infty}[P_{A_0,A_1,A_2,M_0,E_0}]M_{P_{A_0,A_1,A_2,M_0,E_0}}} \quad \text{(A11)}$$

with

$$M_{P_{A_0,A_1,A_2,M_0,E_0}} = (M_0 + E_0 + 1)78 + 16A_0 + 46A_1 + 76A_2 + 44M_0 + 74E_0 \quad \text{(A12)}$$

where $M_{P_{A_0,A_1,A_2,M_0,E_0}}$ is the molar mass of P_{A_0,A_1,A_2,M_0,E_0}; and 78, 16, 46, 76, 44, and 74 g/mol are the molar masses of C_3N_3 (i.e. M without the three amine groups), A_0, A_1, A_2, M_0, and E_0, respectively.

Assuming that amine H's contained in bridges do not undergo methylolation, any P_{A_0,A_1,A_2,M_0,E_0} species contains ($2A_0 + A_1$) reactive H's and ($A_1 + 2A_2$) methylols. Thus, the number-average functionalities of H's, methylols, and (methylene and ether) bridges are:

$$\bar{f}_H = \frac{\sum_{E_0=0}^{\infty}\sum_{M_0=0}^{\infty}\sum_{A_2=0}^{\infty}\sum_{A_1=0}^{\infty}\sum_{A_0=0}^{\infty}\{2A_0 + A_1\}[P_{A_0,A_1,A_2,M_0,E_0}]}{\sum_{E_0=0}^{\infty}\sum_{M_0=0}^{\infty}\sum_{A_2=0}^{\infty}\sum_{A_1=0}^{\infty}\sum_{A_0=0}^{\infty}[P_{A_0,A_1,A_2,M_0,E_0}]} \quad \text{(A13)}$$

$$\bar{f}_{\text{meth}} = \frac{\sum_{E_0=0}^{\infty}\sum_{M_0=0}^{\infty}\sum_{A_2=0}^{\infty}\sum_{A_1=0}^{\infty}\sum_{A_0=0}^{\infty}(2A_2+A_1)[P_{A_0,A_1,A_2,M_0,E_0}]}{\sum_{E_0=0}^{\infty}\sum_{M_0=0}^{\infty}\sum_{A_2=0}^{\infty}\sum_{A_1=0}^{\infty}\sum_{A_0=0}^{\infty}[P_{A_0,A_1,A_2,M_0,E_0}]} \tag{A14}$$

$$\bar{f}_{\text{MB}} = \frac{\sum_{E_0=0}^{\infty}\sum_{M_0=0}^{\infty}\sum_{A_2=0}^{\infty}\sum_{A_1=0}^{\infty}\sum_{A_0=0}^{\infty}M_0[P_{A_0,A_1,A_2,M_0,E_0}]}{\sum_{E_0=0}^{\infty}\sum_{M_0=0}^{\infty}\sum_{A_2=0}^{\infty}\sum_{A_1=0}^{\infty}\sum_{A_0=0}^{\infty}[P_{A_0,A_1,A_2,M_0,E_0}]} \tag{A15}$$

$$\bar{f}_{\text{EB}} = \frac{\sum_{E_0=0}^{\infty}\sum_{M_0=0}^{\infty}\sum_{A_2=0}^{\infty}\sum_{A_1=0}^{\infty}\sum_{A_0=0}^{\infty}E_0[P_{A_0,A_1,A_2,M_0,E_0}]}{\sum_{E_0=0}^{\infty}\sum_{M_0=0}^{\infty}\sum_{A_2=0}^{\infty}\sum_{A_1=0}^{\infty}\sum_{A_0=0}^{\infty}[P_{A_0,A_1,A_2,M_0,E_0}]} \tag{A16}$$

Finally, the global concentrations of reactive H's and methylols are:

$$[-\text{H}] = \sum_{E_0=0}^{\infty}\sum_{M_0=0}^{\infty}\sum_{A_2=0}^{\infty}\sum_{A_1=0}^{\infty}\sum_{A_0=0}^{\infty}\{2A_0+A_1\}[P_{A_0,A_1,A_2,M_0,E_0}] \tag{A17}$$

$$[-\text{CH}_2\text{OH}] = \sum_{E_0=0}^{\infty}\sum_{M_0=0}^{\infty}\sum_{A_2=0}^{\infty}\sum_{A_1=0}^{\infty}\sum_{A_0=0}^{\infty}(2A_2+A_1) \times [P_{A_0,A_1,A_2,M_0,E_0}] \tag{A18}$$

References

1. Wirpsza, Z.; Kucharski, M.; Lubczak, J. J Appl Polym Sci 1998, 67, 1039.
2. Walker, J. F. Formaldehyde, 3rd ed.; Robert E Krieger Publishing Company Huntington: New York, 1964.
3. Gordon, M.; Halliwell, A.; Wilson, T. J Appl Polym Sci 1966, 10, 1153.
4. Okano, M.; Ogata, Y. J Am Chem Soc 1952, 74, 5728.
5. Nastke, R.; Dietrich, K.; Reinisch, G.; Rafler, G. J. Macromol Sci-Chem 1986, A23, 5,579.
6. Nusselder, J. J. H.; TIS28V0, Skill Centre Melamine.
7. Scheepers, M. L.; Adriaenses, P. J.; Gelan, J. M.; Carleer, R. A.; Vanderzande, D. J.; De Vries, N. K.; Brandts, P. M. J Polym Sci Polym Chem 1995, 33, 915.
8. Tomita, B. J Polym Sci 1977, 15, 2347.
9. Nicolau, V.; Estenoz, D.; Meira, G. J Appl Polym Sci 2007, 106, 2978.
10. Nicolau, V.; Estenoz, D.; Meira, G. J Appl Polym Sci, to appear.
11. Gupta, S. K. J Appl Polym Sci 1986, 31, 2805.
12. Kumar, A.; Chandra, R. Polym Eng Sci 1987, 27, 925.
13. Kumar, A.; Katiyar, V. Macromolecules 1990, 23, 3729.
14. Melamine Chemicals.Melamine Crystal: Properties, Chemistry, Analytical Methods, Toxicology; Melamine Chemicals Inc: Donalsonville, LA 70346, USA, 1980.
15. Siling, M. I.; Akselrod, B. Ya Russ J Phys Chem 1968, 42, 1479.